3.3kW Onboard Battery Chargers for Plug-in Vehicles: Specifications, Topologies and a Practical Example

Saeid Haghbin and Torbjörn Thiringer
Electric Power Engineering, Chalmers University of Technology, Gothenburg, Sweden
Emails: {saeid.haghbin, torbjorn.thiringer}@chalmers.se

Abstract—**Battery chargers are essential components for further development of plug-in vehicles including electric or hybrid electric vehicles. The 3.3kW battery charges are widely used in plug-in vehicles in which the power source is the single phase ac grid. The auto industry has stringent requirements on the size, efficiency, temperature and packaging of the onboard chargers that are reviewed in this paper. Usually there is a power factor pre-regulator and an isolated DC/DC stage in a typical onboard charger. Different circuit topologies are feasible for both stages. Some of the most used topologies are reviewed in this paper. Some simulation results are provided and a practical example is presented. Different practical aspects of these chargers are presented and explained.**

Index Terms—**3.3kW onboard battery charger, plug-in vehicles, power factor control, DC/DC converter, interleaved Boost rectifier**

I. Introduction

The concept of more electric transport systems is booming because of several reasons. At one side, there is an increasing demand on energy consumption that needs sustainable solutions to control the environmental adverseness. At the other side the available technology enables us to utilize more electric solutions in traction applications. The passenger car is one of the areas undergoing intensive electrification in different forms. Powertrain and auxiliary systems are heavily investigating to reach the targets set by governments, research institutes and so on. However, the battery price is still a bottleneck to have a fully battery powered powertrain in vehicle applications.

Plug-In hybrid electric vehicles (PHEVs) are an interesting solution to overcome zero emission requirements in the city area and high price of fully electric vehicles. The battery capacity is usually less than 20kWh in a PHEV providing of driving fully electric in a range of 50 km.

Battery chargers have an important impact on the development of plug-in vehicles. They can be a standalone unit out of vehicle with a high power charge capability or an onboard charger with a rated power of 3.3kW. A fast charger with a power level of 100kW may cost more than 100,000USD which enabling battery charging of a typical PHEV in 5-10 minutes [1]. A 3.3kW charger can charge a 20kWh depleted battery pack in less than five hours. At the moment, the price of a 3.3kW onboard battery charger is 500-800USD that makes it interesting solution for auto industry.

The battery charger is the bridge between the grid and the vehicle; this tie imposes requirements on the charger specifications towards the grid and automobile [2]-[9]. It is expected to have the near unity power factor (PFC) operation and stay under certain level of harmonics [2]. Moreover, the charger should withstand the transients and under or over voltage operation [3], [4]. The auto industry requires a high power density efficient charger that could tolerate extreme temperature or vibrating environment with a low price. Despite the fact that electrical isolation is not required by related standards, but for safety reasons it is strongly recommended or required for a charger with a power level of 3.3kW in vehicle applications [6].

After this introduction the typical specifications of a 3.3kW battery charger is presented. Different requirements and expected performance like efficiency and volume are discussed in detail.

There are two stages in a battery charger in this application [10]-[13]: a unity power factor pre-regulator and an isolated DC/DC stage. Section III is dedicated to pre-regulator stage. For instance an interleaved Boost converter can be used in this stage. Different solutions for this AC/DC converter are discussed including some simulation results for an interleaved Boost converter with an average current mode control strategy.

The isolated DC/DC stage is discussed and explained in Section IV. For the DC/DC converter, transformer isolated resonance converter or zero voltage switching (ZVS) Full-bridge converters are usually utilized. Different topologies are discussed and typical simulation results for a Full-bridge converter are presented in this section.

Volvo Car Corporation recently introduced a PHEV which is named V60 model. The battery pack used in V60 is lithium-ion type with the energy of 11.2kWh. A 3kW onboard charger is used in this vehicle. There is a PFC stage and an isolated DC/DC converter with resonance topology in the battery charger. More detailed

Manuscript received January 6, 2015; revised April 16, 2015.

explanations are provided in Section V. The conclusion is the last section of the article, Section VI.

II. The Main Specifications of Onboard 3.3 kW Batrrey Chargers

The main specifications of a typical onboard 3.3 kW battery charger are summarized in Table I [10]-[13].

TABLE I. SPECIFICATIONS OF THE 3.3 KW CHARGER

Parameter	Value
Input voltage from grid utility (single-phase)	85-270 V
Maximum value of input current from the grid	16 A
Ac line frequency range	47-70 Hz
Power factor	More than 99%
Total harmonics distortion (THD)	Less than 5%
Output dc voltage (depend on battery voltage)	200-470 V
Output dc voltage ripple	Less than 2 V
Maximum output dc current	11 A
Maximum output power	3.3 kW
Charger efficiency	Around 94%
Cooling	Liquid
Coolant temperature	-40 to +70 ^{o}C
Ambient temperature	-40 to +105 ^{o}C
Weight/Volume	Around 6Kg/5L

Usually the power level is limited by available power from the utility grid. For instance, the maximum power available from a 220V/16 A is 3520W. Considering the 94% efficiency, the output power is 3.3kW. From the design perspective, the input voltage may have a wide range, as is indicated in the table, but the maximum line current is around 16A. So the charger loads the grid with 16A implying a variable power for different voltage levels.

The near unity power factor and small value of THD is easily achieved by using an active pre-regulator stage including some line filters. The electro magnetic compatibility (EMC) issue is another concern regarding the grid-connected charger. There are plenty of standards covering the EMC and other similar topics like surge transients. For instance one can refer to the IEC 61000-4 [4] series including some of these requirements. However, using a line filter to reduce EMC and transients is the main solution to fulfill these requirements [7]-[9]. The filter design and its optimality will be shortly discussed in the next section.

The nominal battery voltage in a passenger car can be around 300V or 700V. The tendency is towards higher values because of lower current in conductors. However, insulation in devices and equipment makes it difficult to have higher values. For a battery pack with a nominal voltage of 300V, still the battery voltages variations are wide. For example, for a battery pack with nominal value of 300V, the battery voltage can vary between 275-400V depend on the state of charge (SOC).

The charging profile of a battery has three stages. The first stage is the bulk charge that a constant high current is injected to the battery. In this stage the battery will be powered up to the 80% of its capacity. The next stage is called absorption stage in which an absorption voltage is applied to the battery to fill the rest of 20%. The current level is usually low in this stage; and finally the float stage that the battery is kept charged by applying a lower voltage and current compared to the absorption stage.

The impact of the charging profile on the charger is that the designer shall size the conductors for high current charging (bulk) and adjust the transformer turns ration in the DC/DC converter to be able to reach the desired output voltage for absorption stage. Consequently, the maximum current of the charger is not occurring simultaneously with highest voltage. For instance according to Table I, the charger maximum power can be 11A*470V=5170W but this is not the case, and the maximum power is 11A*300V=3300W.

The charger efficiency is an important requirement especially when it directly deals with the customer. The state of art of the available technology for power electronic devices enables an efficiency level of around 94%. The efficiency of the pre-PFC regulator stage is around 98% and for the isolated DC/DC converter it can be around 96%. However, this performance level is reported around nominal power with the input voltage around 230V. Deviations from this input voltage level or charging level reduces the charger efficiency. This issue will be discussed further in the sequel.

The power density is another requirement that is equivalent to the weight and volume. This requirement is extremely important for auto makers because of lack of space in the vehicle. To achieve a higher power density, the current trend is to use liquid cooling, for instance with water, to have a compact package. The power electronics cooling system is usually independent of the vehicle cooling system and it is subject of research to unite vehicle and power electronics cooling.

The vehicle environment is harsh in terms of temperature variations and vibrations. As is indicated in Table I, the ambient temperature can be somewhere between -40- to 105 ℃. It is desirable to have a vehicle to be able to operate in different climate conditions from north of Sweden to dessert area in the middle of Iran, for example.

The highly vibrating environment of a vehicle requires special consideration in packaging and installation of the battery charger. For instance, there is a risk of component disconnection or loose connection over time. This affects the device reliability and probability of failure. Usually the charger is enclosed inside a metallic closure and there are some bumpers to reduce the impact of vibration. In addition, mechanical installation of the components is designed to withstand relative requirements and standards.

III. Input Filter and Unity Power Factor Preregulator

The ideal PFC pre-regulator emulates the converter as a resistor towards the utility grid and transforms the ac power to the charger as a resistor [14]. It is more convenient to approach the power balance for the modeling and control of the converter. Fig. 1 shows the power in different parts of the system. The parameters $P_s(t)$, $P_c(t)$ and $P_L(t)$ are instantaneous power in the source in the converter and the load, subsequently. As is shown in this figure, the converter should be able to store/supply a minimum level of power that is the difference between the constant load power and instantaneous input power. Consequently, this put a limit on the minimum energy storage on the converter that is dc bus capacitor in this case. The dc bus capacitor has a considerable impact on the converter power density; dc bus capacitor reduction is still subject of research to improve the converter power density.

There are different circuit topologies that can be utilized as the PFC pre-regulator. However, the Boost converter is one the most used option for this application. There are different varieties and improvements to the basic Boost converter to achieve closer performance to the ideal AC/DC converter.

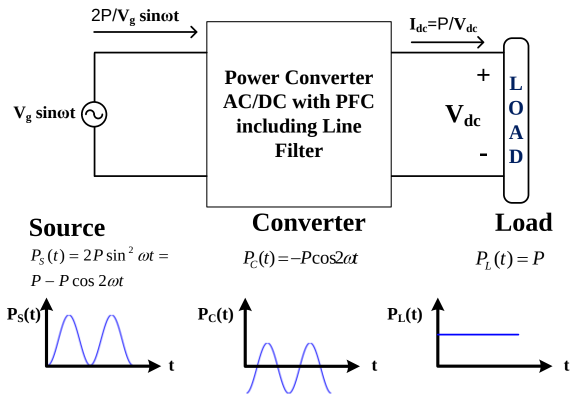

Figure 1. Power balance in an ideal AC/DC PFC converter.

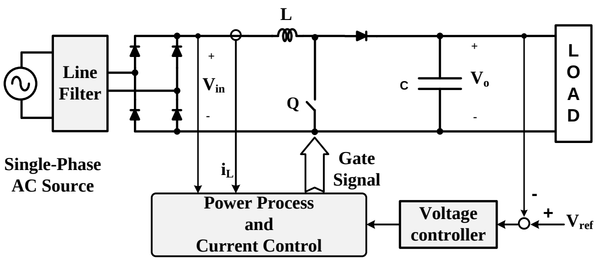

Figure 2. Power rectification with PFC based on Boost topology.

A. Basic Boost Converter

The basic schematic diagram of a Boost converter in a PFC application is shown in Fig. 2. The ac line voltage is rectified by a bridge rectifier. The switch Q that can be a Mosfet for instance, charges the inductor and transfer the power to the output capacitor by a proper switching operation. The inductor is in series with the line impedance that makes it easier to reduce the switching harmonics.

There are two control loops [15]-[22]: an output voltage controller and an inner current controller. The voltage loop is slower than the inner current controller. The bandwidth of the voltage control loop is around 2-20Hz and the bandwidth of the current controller is much faster, that could be around 1/6 switching frequency [22]. It is intended to have a constant output voltage, but there is a voltage ripple determined by the switching frequency and components values. The task of voltage control loop is to program the input current to have a constant power with the unity power factor from the ac source. The deviation from reference output voltage indicates extra energy or energy deficit in the system in which the current level is adjusted by the controller.

Different control strategies have been proposed for the Boost converter in PFC application [22]. The voltage loop is usually a PI controller or type II controller. The output of the voltage controller is the reference value for the current controller. However, there are some enhancements like feedforwad terms to improve the load and line dynamics. The boost converter can operate on three modes depending on the inductor current: continuous conduction mode (CCM), discontinuous conduction mode (DCM) and boundary conduction mode BCM) [23], [24]. In CCM the inductor current will not reach to zero when the current is at its peak value, but in discontinuous mode the inductor current is zero for a while during each switching period. The BCM is the critical point which CCM turns into to DCM. The design rule for inductor value is different for CCM and DCM.

The inductor value for CCM can be determined as [23]

$$L_{CCM} = \frac{V_o}{4f_s\Delta I} \tag{1}$$

where V_o, f_s and ΔI are output voltage, switching frequency and designed current ripple in the inductor consequently. The inductance value for DCM can be determined as [23]

$$L_{DCM} = \frac{V_g(1-\frac{V_g}{V_O})}{f_s\Delta I_P} \tag{2}$$

where V_g is the maximum line voltage and ΔI_P is the current ripple in maximum line current value. The output voltage ripple is

$$\Delta V_o = \frac{P}{2\omega V_o C_o} \tag{3}$$

where ω, and C_o are line angular frequency and dc bus capacitor. P is the output power in this equation.

Despite the converter operation mode, there are different ways for current control inside the fast inner loop. The average current mode control, peak current mode control and boundary current mode control are the main current mode control schemes. All of these three schemes are used for different applications and there are commercially available controllers. The average current mode control (ACMC) [22] is dominant method for high power applications because of its robustness to noise and its stable operation; there is no problem with instability for the duty cycles more than 0.5 as is the case for the peak current mode control.

B. Efficinecy of the Basic Boost Converter

There are mainly two types of losses in the basic Boost converter, semiconductor loss and inductor loss. The input bridge diodes, Mosfet and output diode are the semiconductor switches that have conduction loss and switching loss. In general, semiconductor loss calculation can be very complicated depending on required accuracy [25]-[29].

The inductor loss includes copper loss and core loss. Usually around 0.5% of the total loss is the inductor loss and around 1.5% is semiconductor losses. However, there are other losses like losses in capacitors or line filter devices that have a minor impact on the loss analysis.

The input bridge rectifier includes four diodes which two of them are conducting simultaneously. The switching loss is negligible and the conduction loss can be calculated by considering the diode on resistance and forward voltage drop for a specific value of the current. For example, with a 16A rms input current and with a 1V voltage drop, the loss in one diode can be calculated as $\frac{2}{\pi}I_P=\frac{2}{\pi}16\sqrt{2}=14.4$W. For two diodes the loss is 28.8W. So the input bridge loss is around 28.8W that is around 0.1% of total loss in nominal condition. The average value of the fast diode is the same as the output dc current. If the switching loss is negligible for the fast diode, for instance by utilizing SiC materials, the loss is $I_{dc}V_f$. For example for a typical diode this can be 11A*1V=11W. The Mosfet loss, switching and conduction, has not a straightforward calculation method. Usually, circuit simulator generates ideal waveforms to be used by another program to calculate the loss. The datasheet information is extracted to be able to perform loss calculations for Mosfet.

C. Interleaved Boost Converter

The interleaved Boost converter is an interesting topology from the Boost converter family providing interesting advantages over basic converter [23], [24], [30]-[33]. There are two energy storage inductors with two independent switches and diodes that share the same bridge rectifier at the input side and the same dc bus capacitor, as is shown in Fig. 3. The switching functions are interleaved which significantly reduces the input line and output ripples. It simply can reduce the ripple to half when the duty cycle is half. In addition, interleaving provides the capability of parallel converter operation for higher power applications. The idea of interleaving is that two inductors have opposite ripple directions; and they cancel out each other in the line current.

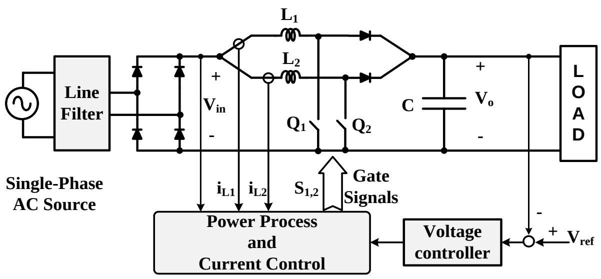

Figure 3. Interleaved Boost rectifier as the frontend converter.

For a converter with a power level of 3.6kW at the input side, the line current and voltage are shown in Fig. 4 where a step change in load from half to full load is applied at t=1.5s. The switching frequency in this case is 70kHz. The converter dc voltage is shown in Fig. 5 for a similar situation.

This circuit topology has been employed in several 3.3 kW battery chargers as the front end PFC pre-regulator stage. The converter has higher efficiency compared to the classical Boost converter that will be discussed in this section later on.

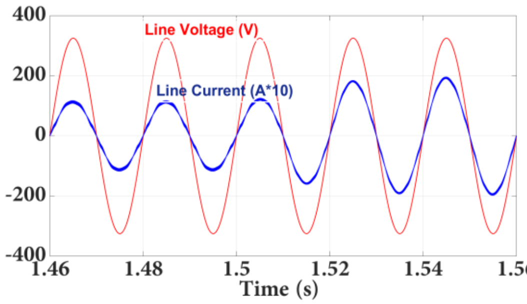

Figure 4. Simulation result: line current and voltage in interleaved Boost rectifier (response to step-change in load).

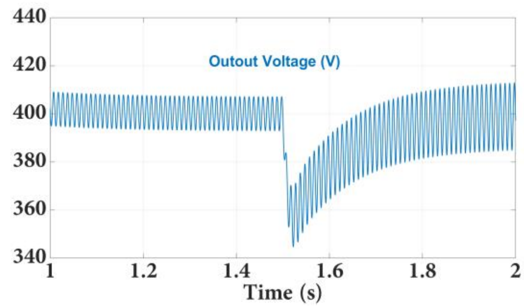

Figure 5. Simulation result: output dc in interleaved Boost rectifier (response to step-change in load).

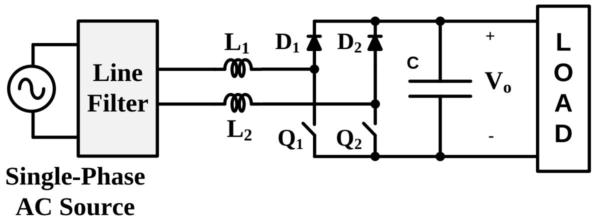

Figure 6. Bridgeless boost rectifier as the frontend converter

D. Bridgless Converter

To achieve higher efficiencies and lower component numbers, the Bridgeless converter is proposed as a viable alternative for the PFC pre-regulator [30]. Fig. 6 shows the converter topology. As can be seen from the figure the input bridge is eliminated. However, the main limitation with this topology is increased noise towards the utility grid leading to a need of more filtering. Considering the filter, this topology may not be an interesting solution for PFC applications.

E. Regulatory Standards and Line Filters

For the grid connected chargers there are two types of regulatory standards: standards addressing harmonics (lower frequency range) and standards dealing with higher frequencies concerning EMC. The main objectives of low frequency standards like IEC 6100-3-2 [2] are power factor, harmonics and THD. Above mentioned

Boost topologies will easily pass the low frequency requirements if they operate properly. However, it is more challenging to cope with EMC issues.

There are standards concerning higher frequencies like IEC 61851-21-1 [3] that is dedicated to onboard battery chargers in vehicle applications. The frequency range of the standards addressing EMC is 150kHz-30MHz. The high frequency noise is around the switching frequency and its multiples. For instance, one can choose the switching frequency lower than 150kHz to be under the 150kHz limit. However, a line filter shall be utilized to make sure that the device can fulfill this requirement. Both the common mode noise and differential mode noise should be considered in filter design.

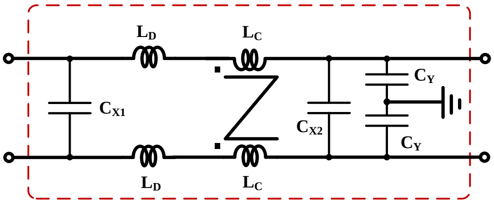

Figure 7. Typical EMI filter to fulfill standard requirement regarding high frequency noise.

Fig. 7 shows a typical EMI filter where there are differential mode filtering and common mode filtering stages [34]. In addition, there might be some protective devices like voltage suppressors or surge arrestors to cope with transients.

The filter has an important impact on the total power density; it is ideal to optimize the filter and PFC pre-regulator to have even better performance in terms of power density. For instance, one can reduce the size of Boost inductor which would give a higher current ripple. This can be compensated by have a larger filter. So, it an optimization question to find out a proper compromise between the filter and PFC pre-regulator. In this paper, the optimization is not performed, but it is referred to previous works to cover the topic [20].

IV. Isolated DC/DC Converter

The second stage of the battery charger is the DC/DC conversion with galvanic isolation. In general, depending on the power level and utilized technology, like inductive or conductive charging, there are different topologies for this stage that one can read a comprehensive review in [12]. However, for the power level of 3.3kW with high-power density requirement, the Full-bridge topology is one of the mostly used configurations. To increase the power density to the target level (refer to Table I) it is inevitable to have a higher switching frequency, for instance around 200kHz.

High-frequency operation of the converter poses increased switching losses in semiconductors and magnetic losses; naturally configurations with soft-switching like zero voltage switching (ZVS) and/or zero current switching (ZCS) will be highlighted. Transformer-isolated soft-switched Full-bridge topology and its variations are the main candidates; there are two main families of Full-bridge topologies [35]: soft-switched topologies and resonance topologies. Resonant converters are inherently soft switched topologies.

The resonant converter has slightly higher efficiency compared to the Full-bridge with ZVS but the semiconductors have more stress. In addition, the frequency control is used in resonance converters that makes it complicated compared to fixed frequency control of Full-bridge with ZVS. These two configurations are briefly discussed in the sequel.

A. Full-Bridge Topology with ZVS

Fig. 8 shows the power stage of a Full-bridge converter with ZVS operation [36]. There are four switches in two legs converting DC voltage to high-frequency AC voltage. The input DC voltage is the output of the PFC stage. The transformer provides galvanic isolation and voltage ratio adjustment. The transformer output is rectified by a diode-bridge and then an LC filter smoothes the output voltage. Usually a T-model of the transformer is used in the modeling that includes primary leakage inductance, magnetizing inductance and secondary leakage inductance (Fig. 8). The main idea of the soft switching is to deploy the stored energy in the switches capacitors to the source by utilizing the leakage inductance of the transformer. However, both capacitors and leakage inductor can be external components.

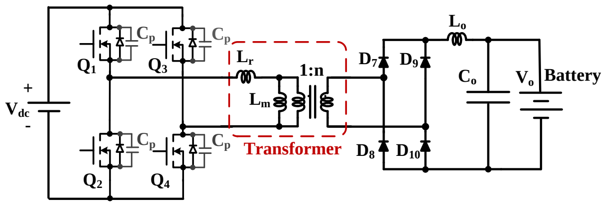

Figure 8. The power stage of a Full-bridge transformer isolated converter with ZVS.

The switching frequency is constant and by utilizing the stored energy in the leakage inductor, it is intended to deploy the stored energy in switches capacitor to reduce the switching loss.

Silicon-Carbide (SiC) devices are known as wide bandgap semiconductors suitable for fast switching and high temperature environment. Recently they have gained attention and several applications have been reported in this regard. The switching loss can be dramatically reduced by utilizing SiC semiconductors. However, conduction losses could be higher than similar devices, i.e. Si-based [25]-[29].

There are different ways to control four switches at input bridge; if the top and bottom switches have constant duty cycle, 50% each, by controlling the phase shift between two legs, one can control the output voltage. This is the phase-shifted ZVS Full-bridge topology. The main feature of this structure is the constant frequency operation. A maximum efficiency of 96% is typical with this configuration.

At light loads, the stored energy in the leakage inductor is lower than the stored energy in the switches capacitors, so the ZVS operation is not feasible. This is a design tradeoff and usually up to 50% of nominal load is selected by the designer. Below this value the converter efficiency is lower than the nominal condition.

B. *Resonant Full-Bridge Topology with LLC Configuration*

Inductor-Inductor-Capacitor (LCC) resonant converter is one of the attractive alternatives as DC/DC converter because of high efficiency, high power density, lower EMI levels and wide operation ranges [37]. The waveforms are sinusoidal during one or more subinterval of each switching period [35]; so the small signal approximation is not valid for the resonance converters.

Fig. 9 shows the power stage of a transformer isolated LLC resonant converter in which the resonant tank is specified in the figure. The input bridge provides a square waveform with a controllable frequency around 80kHz for example. The resonant tank includes C_r, L_r and L_m which are a series capacitor, the transformer leakage and magnetization inductances consequently; the transformer adjusts the voltage level for the bridge and output low pass filter. The full analysis of the resonant converter is not a straightforward task. However, with some simplifications it is possible to have an acceptable design procedure. If the main component of the bridge output voltage is considered, then one can analyze the circuit based on the phasor method.

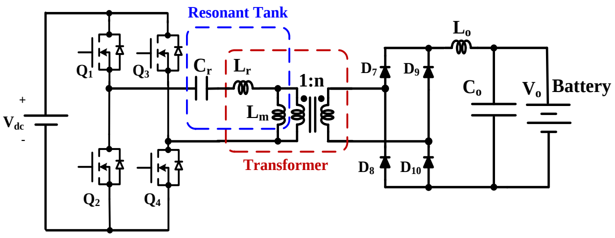

Figure 9. The power stage of an isolated Full-bridge LLC resonant converter.

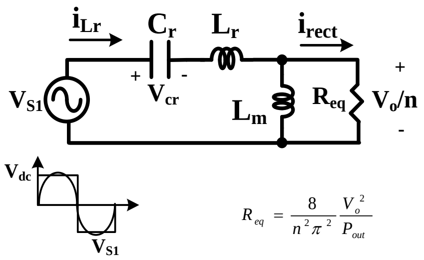

Figure 10. Equivalent circuit of the LLC resonant converter considering the fundamental component.

Fig. 10 shows the equivalent circuit diagram of the LLC converter considering just the first harmonic. The output rectifier and filter is modeled as an equivalent resistor [35] considering the transformer turns ratio, n. The equivalent resistance from the primary side is $R_{eq}=\frac{8}{n^2\pi^2}\frac{V_o^2}{P_{out}}$, where V_o and P_{out} are the output voltage and power respectively.

By controlling the bridge frequency, the resonant tank shows different impedances, which is the mechanism to regulate the output voltage. However, the frequency variation can't be extremely wide in order to violate the first harmonic assumption. The next harmonic of the bridge square wave is the third one. The variable frequency control is apparently a negative point compared to the fixed switching frequency controlled schemes, especially when it comes to digital implementation.

As is mentioned earlier, the output battery voltage has a wide range that can be from 275-400V which makes it challenging to design the controller especially considering ZVS or ZCS operation. The best efficiency of 98% [37] is reported for this circuit and it turns out that it is a viable option for battery charging. At lighter load the ZVS is not performed that reduces the efficiency of the charger [37].

V. Practical Example of the Onboard Battery Charger Used in Volvo Car V60

The Norway-based Eltek Company supplied onboard battery chargers to Volvo Car Corporation to be used in the V60 PHEV. The charger is a water cooled device installed in an aluminum enclosure. The CAN controller in the charger unit provides the communication protocol.

The charger is installed in two different mechanical enclosures: one with ingress protection (IP) 20 and another one with IP 67. The device with IP 20 weights 2.8kg and the one with IP 67 weights 4.3kg. The power density in the first case is 1.8kW/liter, which is very high. Table II provides a summary of the charger specification.

TABLE II. Specifications of the Eltek 3kW Charger [38]

Parameter	Value
Input voltage from grid utility (single-phase)	85-275 V
Maximum value of input current from the grid	14 A
Ac line frequency range	45-65 Hz
Power factor	More than 99%
Total harmonics distortion (THD)	Less than 5%
Output dc voltage	250-420 V
Output dc voltage ripple	Less than 2 V
Maximum output dc current	10 A
Maximum output power	3 kW
Charger efficiency	96% at 50% load 95% at 100% load
Applicable standards Electrical safety EMC: immunity, light industry EMC: immunity, industry EMC: emission, light industry EMC: emission, industry Mains Harmonics	 IEC 61851-1 EN 61000-6-1 EN 61000-6-2 EN 61000-6-3 EN 61000-6-4 EN 61000-3-2
Cooling	Liquid
Operating temperature	-40 to +60 °C
Dimensions	49x280x120mm (IP20) 60x355x167mm (IP67)
Weight	2.8 kg (IP20) 4.3 kg (IP67)

VI. Conclusions

3.3kW battery chargers are a favorable alternative by auto industries for PHEVs. Different requirements of such a charger like power density and efficiency are explained in this paper. The charger has two converter stages: an AC/DC pre-regulator stage and an isolated DC/DC converter. Interleaved Boost converter is a potential topology for the pre-regulator stage. The ZVS Full-bridge topology and the LLC resonant topology are the main candidates for the DC/DC stage.

Acknowledgment

The financial support given by Energimyndigheten (Swedish Energy Agency) is gratefully acknowledged.

References

[1] S. Haghbin, "Integrated motor drives and battery chargers for electric or plug-in hybrid electric vehicles," PhD thesis, Chalmers University of Technology, Sweden, 2013.

[2] Limits for Harmonic Current Emissions (Equipment Input Current <16A per Phase), IEC61000-3-2, Aug. 1995.

[3] Electric Vehicle Conductive Charging System - Part 21-1 Electric Vehicle Onboard Charger EMC Requirements for Conductive Connection to a.c./d.c. Supply, IEC 61851-21-1, 2013.

[4] Electromagnetic Compatibility Series, IEC 61000-4.

[5] S. Basu, M. H. J. Bollen, and T. M. Undeland, "PFC Strategies in light of EN 61000-3-2," *APEC Paper A*, 2005.

[6] A. Di Napoli and A. Ndokaj, "EMC and safety in vehicle drives," in *Proc. 14th European Conference on Power Electronics and Applications (EPE 2011)*, 2011, pp. 1-8.

[7] J. Muhlethaler, H. Uemura, and J. W. Kolar, "Optimal design of EMI filters for single-phase boost PFC circuits," in *Proc. 38th Annual Conference on IEEE Industrial Electronics Society*, Oct. 2012, pp. 632-638.

[8] F. Yang, X. Ruan, Q. Ji, and Z. Ye, "Input differential-mode EMI of CRM boost PFC converter," *IEEE Transactions on Power Electronics*, vol. 28, no. 3, pp. 1177-1188, Mar. 2013.

[9] J. C. Crebier and J. Ferrieux, "PFC full bridge rectifiers EMI modeling and analysis-common mode disturbance reduction," *IEEE Transactions on Power Electronics*, vol. 19, no. 2, pp. 378-387, Mar. 2004.

[10] M. C. Kya, "Design, implementation, and control of a two stage AC/DC isolated power supply with high input power factor and high efficiency," PhD thesis, Middle East Technical University, 2013.

[11] K.-W. Koo, D.-H. Kim, D.-G. Woo, and B.-K. Lee, "Topology comparison for 6.6kW on board charger: Performance, efficiency, and selection guideline," in *Proc. IEEE Vehicle Power and Propulsion Conference (VPPC)*, Oct. 2012, pp. 1520-1524.

[12] A. Khaligh and S. Dusmez, "Comprehensive topological analysis of conductive and inductive charging solutions for plug-in electric vehicles," *IEEE Transactions on Vehicular Technology*, vol. 61, no. 8, pp. 3475-3489, Oct. 2012.

[13] D. S. Gautam, F. Musavi, M. Edington, W. Eberle, and W. G. Dunford, "An automotive onboard 3.3-kW battery charger for PHEV application," *IEEE Transactions on Vehicular Technology*, vol. 61, no. 8, pp. 3466-3474, Oct. 2012.

[14] Power Electronics Group, California Institute of Technology, "Input-Current shaped ac-to-dc converters," NASA Report Number N86-25693, May 1986.

[15] H. Y. Kanaan, G. Sauriol, and K. Al-Haddad, "Small-Signal modelling and linear control of a high efficiency dual boost single-phase power factor correction circuit," *IET Power Electronics*, vol. 2, no. 6, pp. 665-674, Nov. 2009.

[16] J. B. Williams, "Design of feedback loop in unity power factor AC to DC converter," in *Proc. 20th Annual IEEE Power Electronics Specialists Conference*, Jun. 1989, pp. 959-967.

[17] R. D. Middlebrook, "Small-Signal modeling of pulse-width modulated switched-mode power converters," *Proceedings of the IEEE*, vol. 76, no. 4, pp. 343-354, Apr. 1988.

[18] P. Cooke, "Modeling average current mode control [of power convertors]," in *Proc. Fifteenth Annual IEEE Applied Power Electronics Conference and Exposition*, 2000, pp. 256-262.

[19] W. Tang, F.C. Lee, and R. B. Ridley, "Small-Signal modeling of average current-mode control," *IEEE Transactions on Power Electronics*, vol. 8, no. 2, pp. 112-119, Apr. 1993.

[20] F. A. Huliehel, F. C. Lee, and B. H. Cho, "Small-Signal modeling of the single-phase boost high power factor converter with constant frequency control," in *Proc. 23rd Annual IEEE Power Electronics Specialists Conference*, 1992, pp. 475-482.

[21] R. D. Middlebrook, "Topics in multiple-loop regulators and current-mode programming," *IEEE Transactions on Power Electronics*, vol. PE-2, no. 2, pp. 109-124, Apr. 1987.

[22] L. H. Dixon, "Average current mode control of switching power supplies," Unitrode Application Note, 1990.

[23] K. Raggl, T. Nussbaumer, G. Doerig, J. Biela, and J. W. Kolar, "Comprehensive design and optimization of a high-power-density single-phase boost PFC," *IEEE Transactions on Industrial Electronics*, vol. 56, no. 7, pp. 2574-2587, Jul. 2009.

[24] T. Nussbaumer, K. Raggl, and J. W. Kolar, "Design guidelines for interleaved single-phase boost PFC circuits," *IEEE Transactions on Industrial Electronics*, vol. 56, no. 7, pp. 2559-2573, Jul. 2009.

[25] H. Kragh, F. Blaabjerg, and J. K. Pedersen, "An advanced tool for optimised design of power electronic circuits," in *Proc. Thirty-Third IAS Annual Meeting, Industry Applications Conference*, Oct. 1998, pp. 991-998.

[26] I. K. Budihardjo, Peter O. Lauritzen, and H. A. Mantooth, "Performance requirements for power MOSFET models," *IEEE Transactions on Power Electronics*, vol. 12, no. 1, pp. 36-45, Jan. 1997.

[27] C. L. Ma and P. O. Lauritzen, "A simple power diode model with forward and reverse recovery," *IEEE Transactions on Power Electronics*, vol. 8, no. 4, pp. 342-346, Oct. 1993.

[28] Z. Wang, A. T. Bryant, J. Wu, and P. R. Palmer, "Implementation and comparison of power diode models for system simulation," in *Proc. International Conference on Power Electronics and Drives Systems*, 2005, vol. 1, pp. 694-699.

[29] C. M. Tan and K.-J. Tseng, "Using power diode models for circuit simulations-a comprehensive review," *IEEE Transactions on Industrial Electronics*, vol. 46, no. 3, pp. 637-645, Jun. 1999.

[30] F. Musavi, W. Eberle, and W. G. Dunford, "A high-performance single-phase bridgeless interleaved PFC converter for plug-in hybrid electric vehicle battery chargers," *IEEE Transactions on Industry Applications*, vol. 47, no. 4, pp. 1833-1843, 2011.

[31] F. Musavi, W. Eberle, and W. G. Dunford, "A phase-shifted gating technique with simplified current sensing for the semi-bridgeless AC-DC converter," *IEEE Transactions on Vehicular Technology*, vol. 62, no. 4, pp. 1568-1576, May 2013.

[32] F. Musavi, D. S. Gautam, W. Eberle, and W. G. Dunford, "A simplified power loss calculation method for PFC boost topologies," in *Proc. IEEE Transportation Electrification Conference and Expo (ITEC)*, Jun. 2013, pp. 1-5.

[33] F. Musavi, W. Eberle, and W. G. Dunford, "Efficiency evaluation of single-phase solutions for AC-DC PFC boost converters for plug-in-hybrid electric vehicle battery chargers," in *Proc. IEEE Vehicle Power and Propulsion Conference (VPPC)*, Sep. 2010, pp. 1-6.

[34] M. Pieniz, J. R. Pinheiro, and H. L. Hey, "An investigation of the boost inductor volume applied to PFC converters," in *Proc. 37th IEEE Power Electronics Specialists Conference*, 2006, pp. 1-7.

[35] R. W. Erickson and D. Maksimovic, *Fundamentals of Power Electronics*, 2nd ed., Springer, 2001.

[36] D. Gautam, F. Musavi, M. Edington, W. Eberle, and W. Dunford, "A zero voltage switching full-bridge DC-DC converter for an on-board PHEV battery charger," in *Proc. IEEE Transportation Electrification Conference and Expo (ITEC)*, 2012, pp. 1-6.

[37] J. Deng, S. Li, S. Hu, C. C. Mi, and R. Ma, "Design methodology of LLC resonant converters for electric vehicle battery chargers," *IEEE Trans. on Vehicular Technology*, vol. 63, no. 4, May 2014.

[38] *3kW Traction Battery Charger Module*, Datasheet, Eltek Valere Co.

Saeid Haghbin received his Master degree in electrical engineering from Sharif University of Technology, Iran, in 2003. During 2003-2007 he was working in industry mainly on power electronic systems and automation. He received his PhD degree in Electric Power Engineering

in 2013 from Chalmers University of Technology, Sweden. At the present time he is a postdoctoral fellow at Chalmers University of Technology. His main research interests are power electronics, drive systems and related signal processing.

Torbjörn Thiringer works at Chalmers university of Technology, in Gothenburg Sweden, as a professor in applied power electronics. He took his M.Sc and Ph.D at Chalmers University of technology in 1989 and 1996 respectively. His areas of interest include the modeling, control and grid integration of wind energy converters into power grids as well as power electronics and drives for other types of applications, such as electrified vehicles, buildings and industrial applications.